

Accuracy Assessment of a Photogrammetric UAV Block by using Different Software and Adopting Diverse Processing Strategies

Vittorio Casella¹, Filiberto Chiabrando², Marica Franzini¹ and Ambrogio Maria Manzino³

¹Department of Civil Engineering and Architecture, University of Pavia, Pavia, Italy

²Department of Architecture and Design, Polytechnic of Turin, Turin, Italy

³Department of Environment, Land and Infrastructure Engineering, Polytechnic of Turin, Turin, Italy

Keywords: UAV, Bundle Block Adjustment, Accuracy Evaluation, Open Source Software and Point Clouds.

Abstract: UAVs systems are heavily adopted nowadays to collect high resolution imagery with the purpose of documenting and mapping environment and cultural heritage. Such data are currently processed by programs based on the Structure from Motion (SfM) concept, coming from the Computer Vision community, rather than from classical Photogrammetry. It is interesting to check whether some widely accepted rules coming from old-fashioned photogrammetry still holds: the relation between accuracy and GSD, the ratio between the altimetric and planimetric accuracy, accuracy estimated on GCPs vs that estimated with CPs. Also, not all the SfM programs behave in the same way. To face the envisaged aspects, the paper adopts a comparative approach, as several programs are used, and numerous configurations considered. The University of Pavia established a test field at a sandpit located in the Province of Pavia, in northern Italy, where several flights were performed by the multi-rotor HEXA-PRO UAV, equipped with a 24 MP Sony Alpha-6000. One of these blocks has been extensively analysed in the present paper. The paper illustrates the dataset adopted, the carefully-tuned processing strategies and BBA (Bundle Block Adjustment) results in terms of accuracy for both GCPs and CPs.

1 INTRODUCTION

The use of UAV for surveying purposes (mapping, 3D modelling, point cloud extraction, orthophoto generation) has become a standard operation for the knowledge of the environment and of the built-up areas. The high quality of COTS (Commercial Off-The-Shelf) cameras, easily implemented in UAV platforms, and the development of new programs for image processing created, in the last years, an important revolution in the Geomatics field. We are assisting to a transformation in the photogrammetric community even more connected to the Computer Vision one in terms of algorithms and *rules* for data processing. Starting from these assumptions, the aim of the paper is to analyse from a photogrammetric point of view (according to the *forma mentis* of the authors) the performance of some programs which are today generally employed for processing the data acquired by UAV using the Structure-from-Motion-oriented approach. The tests were performed to carefully assess the accuracies of the final products and to examine the processing steps that usually characterize a traditional photogrammetric workflow such as the Interior Orientation (IO), results

of the Bundle Block Adjustment (BBA), the residuals on the Ground Control Points (GCPs) and Check Points (CPs).

Several papers are connected to the employment of UAV for mapping purpose such as (Zongjian, 2008; Remondino et al., 2011; Lucieer et al., 2014; Samad et al., 2013; Nex and Remondino, 2014) and some analysis of the Bundle Block Adjustment (BBA) connected to traditional photogrammetry are reported in Gini et al. (2013), Nocerino et al. (2013), Benassi et al. (2017) and Verykokou et al. (2018). GCPs configuration also plays a key-role as their number and distribution influence final accuracy as explored by several authors such as Rangel et al. (2018), James et al. (2017) and Tahar (2013).

According to those analysis the paper needs to go in deeper when is possible in the processing steps and in the delivered results connected to the actual software that are commonly used for processing the UAV data for mapping purpose.

The work deals with the data acquired by an UAV flight performed over a sandpit where several points were measured to use within the BBA operation to perform independent check, afterwards. The different followed strategies are accurately described in terms of

weights of the observations used in the adjustment, strategies for tie point extraction and number of GCPs and CPs. Finally, an accurate analysis of the achieved results is reported to understand which are the problem that could be founded during the data-processing and which strategy should be the most suitable for the survey purpose.

2 DATA ACQUISITION

The test-site is a part of a large sandpit located in the Province of Pavia, in northern Italy. The selected area roughly has a horseshoe configuration and is constituted by two flat regions connected by the excavation front, being 10 meters high and having a slope between 30° and 90°. The upper flat zone and the scarp are mainly bare, while the lower one shows a large vegetated area (Figure 1). The surveyed surface is approximal 2 hectares.



Figure 1: Overview of the test site.



Figure 2: The markers.

Before the flights, 18 markers (Figure 2) were positioned and surveyed by an integrated use of classical topography and GNSS, in a redundant way. The GCPs' proper names range from CV1 to CV18. Their coordinates were obtained by least-squares adjustment and their precision is around 0.5 cm for the planimetric components and 1 cm for altimetry. Several photogrammetric blocks were acquired by a UAV equipped with a Sony A6000 camera (Figure 3), under different configurations. The vehicle was made by

an Italian craftsman and has the following main characteristics: 6 engines, Arducopter-compliant flight controller, maximum payload of 1.5 kg (partly used by the gimbal, weighting 0.3 kg), autonomy of approximately 15 minutes.



Figure 3: The HEXA-PRO UAV system operated by the Laboratory of Geomatics at the University of Pavia.

The camera has 24 MP, a focal length of 16 mm and a 17.5 mm GSD at the 70 m flying height. The blocks carried out over the area are all listed in Table 1; the present paper only concerns a dataset coming from the union of blocks 1 and 2, constituted by seven strips. Flying height was about 70 m on average; end lap (longitudinal) and side lap (lateral) were 77% and 60% respectively; more details can be found in (Cassella and Franzini, 2016).

The Pavia group carried out the installation of the markers, their measurement and the UAV missions.

Table 1: List of the various blocks acquired.

Block 1	North-South linear strips, at 70 metres flying height (with respect to the upper part of the site), vertical images
Block 2	East-West linear strips, 70 m, vertical
Block 3	Radial linear strips, 70 m, vertical
Block 4	Radial linear strips, 70 m, 30° inclined
Block 5	Circular trajectory, 30 m, 45° inclined
Block 6	North-South linear strips, 40 m, vertical
Block 7	East-West linear strips, 40 m, vertical
Block 8	Radial linear strips, 40 m, vertical

3 DATA PROCESSING

The University of Pavia and the Polytechnic of Turin decided to process the same dataset with different software they are expert on. The Pavia unit used Agisoft Photoscan and Trimble UAS Master, while in Turin Pix4D, Context Capture by Bentley and MicMac were used. GCPs/CPs configuration was discussed in advance and kept fixed by both groups. Three scenarios were considered, shown by (Figure 5, 6 and 7), according to the criteria listed below;

GCPs are shown in red and CPs in blue:

- Configuration 1 - all the markers are used as GCPs, to perform robust camera calibration (18 GCPs / 0 CPs);
- Configuration 2 - an intermediate setup with strong ground control and still some check points (11 GCPs / 7 CPs);

- Configuration 3 - only 6 points are used as GCPs, that is realistic for routine surveying (6 GCPs / 12 CPs).

Other parameters and configurations were managed independently by the two groups, namely: image alignment, camera calibration and the adjustment weighing. More details can be found in the next sections.

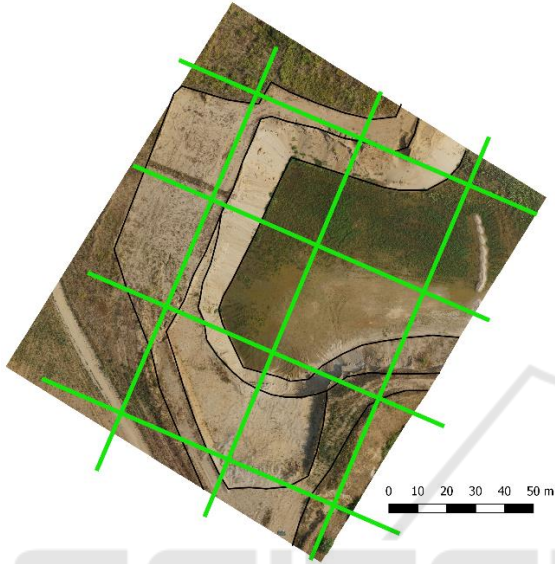


Figure 4: The block structure with three North-South and four East-West linear strips. The images also show black lines accounting for the main morphological features of the sandpit.

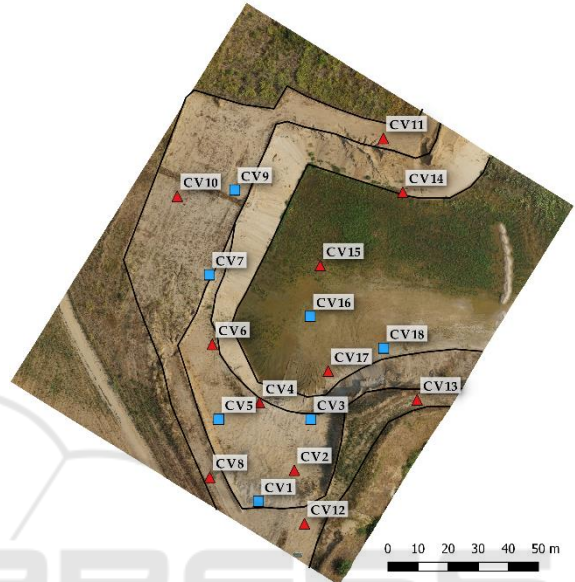


Figure 6: Configuration 2: 11 GCPs for BBA (red triangles) and 7 CPs for quality assessment (blue squares).

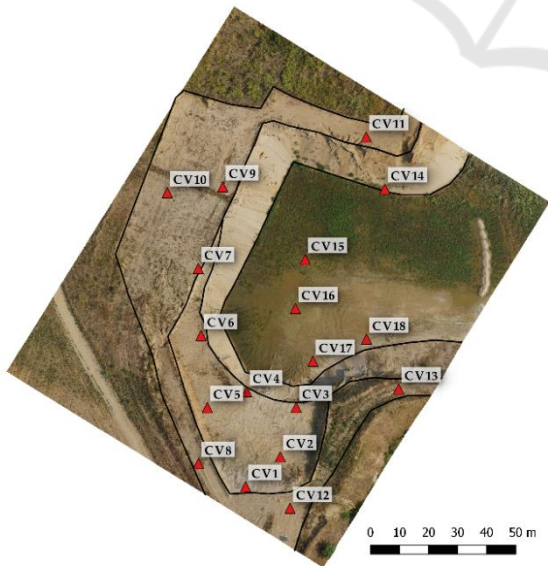


Figure 5: Configuration 1: all the GCPs used for BBA (red triangles).

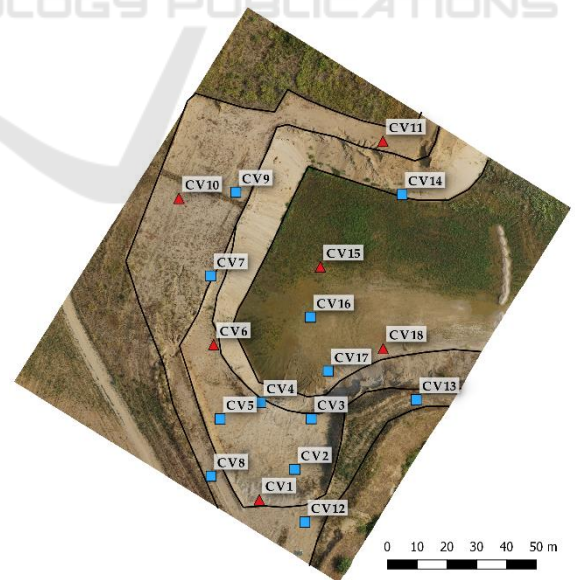


Figure 7: Configuration 3: 6 GCPs for BBA (red triangles) and 12 CPs for quality assessment (blue squares).

3.1 The Unit of the University of Pavia

Data processing was performed with two software: Agisoft Photoscan (rel. 1.2.4) and Inpho UAS Master (rel. 7.0.1). The Photoscan processing will be addressed first.

- When executing the photo alignment, the “High accuracy” setup was chosen, in which tie points were extracted from the full resolution images, while the “Pair preselection” parameter was set on “Generic” since no a-priori information about imagery positions was available.
- Image-point measurement was carried out in a conservative way, meaning that, for each image, only clearly visible points were measured. The average number of measurements per marker was 15 with a minimum of 9 for CV7 and a maximum of 29 for CV17.
- Concerning camera self-calibration, after some testing, it was decided to re-estimate camera interior orientation and to adopt the parameter set proposed as a default by the program. It is constituted by the focal length (f), the corrections for the principal point position (c_x and c_y), the first three coefficients of radial distortion (K_1 , K_2 and K_3) and the first two of tangential distortion (P_1 and P_2). We didn’t insert any approximate values for the camera model, as that didn’t apparently give any benefit.
- Concerning the BBA (Bundle Block Adjustment) weighting strategy, accuracy of ground-coordinates of markers was set at 0.5 cm for the planimetric components and 1 cm for altimetry. For image-coordinates of manually-measured markers, accuracy was set at $\frac{1}{4}$ of the pixel size. Finally, for automatically-measured image-coordinates of tie points, accuracy was set at 1.5 pixels, corresponding to three-times the overall re-projection error. In doing so, we followed the suggestions of the program developers, to be adopted in the case of blurred images; we also verified that the implemented strategy gave the best results in terms of residuals for the CPs.

When UAS Master was used, the same setup was used, with some exceptions. First, the program needs to know approximate external orientation parameters: we supplied the values calculated by PhotoScan. Tie point extraction was performed with the “Full resolution” mode. Image-coordinates of markers were measured by a different operator, with the same style of being conservative and measuring only well visible targets: the mean number of observations was 15 with a minimum of 9 measurements on CV8 and a maximum of 26 on CV17. The parameters for camera self-

calibration are the same as those adopted for PhotoScan. Object-coordinates of markers were weighted as illustrated above, but we were not able to find any interface allowing us to fix the uncertainty of image-coordinates of markers and tie points: we infer that the program applies default values. We must declare that, while we are good experts of Photoscan, we could only use UAS Master for a few months, due to an evaluation license. Even though maximum care was taken, some features of the program could have been overlooked.

3.2 The Unit of the Polytechnic of Turin

The processing was realized using three well known software in the scientific community: the commercial programs Pix4D (2.1.61), Context Capture (4.3.0.507) and the open-source tool MicMac.

The first processing was carried out using Pix4D, where, to follow the most similar approach of the processing steps achieved by the Pavia unit, the following set-up was used:

- For the key point extraction in the initial processing the “Full” option was employed, this settings means that the images were used at the full scale, the matching image pairs according to the input data was set-up for aerial grid and finally, in the calibration options, the parameters were used in the automatic/standard configuration (automatic way to select which key-points are extracted, standard calibration method with an optimization of all the internal parameters (since is well known that the camera used with UAVs, are much more sensitive to temperature or vibrations, which affect the camera calibration, as a consequence it is recommended to select this option when processing images taken with such cameras)). Finally, the rematch option that allows to add more matches after the first part of the initial processing, which usually improves the quality of the reconstruction was used as well (this part is important not in the first alignment but for improving it after the GCPs measurements);
- Image-point measurement was carried out according to the strategy followed by Pavia unit, in this case the average number of measurements per marker was 26 with a minimum of 15 for CV10 and a maximum of 40 for CV17.
- The next step was the BBA (bundle block adjustment), for this step-in order to fix a weighting for the two components, according to the accuracy of the measured coordinates of the

markers the horizontal accuracy was set at 0.5 cm while the vertical accuracy was fixed at 1 cm. It is not possible in Pix4D to set the accuracy of the measurement on the images, probably this value as commonly used is fixed at $\frac{1}{2}$ of the pixel size. During the BBA the camera self-calibration is calculated as well, in this case the parameter set as default has been used. The final results of the camera calibration in Pix4D could be extracted from the final report and are related to the focal length (f), the corrections for the principal point position (cx and cy), the first three coefficients of radial distortion (K1, K2 and K3 called R1 R2 and R3 in Pix4d) and the first two of tangential distortion (P1 and P2 called T1 and T2 in Pix4d).

The second commercial employed software was Context Capture by Bentley System, the approach followed by this program is similar to the one described above and is summarized in the following points:

- The first alignment has been performed using the default setting with “High” density in the key point extraction (scale image size), in this first step the software starting from the information derived by the EXIF file adjust the camera internal parameters as well (f, cx, cy, K1, K2, K3, P1 and P2).
- After the first processing step the camera pose were estimated in an arbitrary coordinate system, the next step was the image-point measurements. In order to help the operator in the measurement phase this part was performed first of all using three GCPs in three different images and then a rigid registration was performed. Starting from this first results an accurate measurement of the other points has been achieved, the average number of measurements per marker was 15 with a minimum of 9 for CV10 and a maximum of 33 for CV17.
- The BBA weighting for the two components, was in the horizontal component 0.5 cm while the vertical one was fixed at 1 cm (the same settings of the other employed commercial software). During the BBA the camera optimization has been performed as well to define the internal parameters of the employed camera.

Furthermore, according to the actual trend in the Geospatial information area that even more move the attention to the open-source software and tools in the presented test the open source software MicMac has been employed. The software has been developed by the MATIS laboratory (IGN France) and it has been delivered as open source in 2007, usable in different contexts (satellite, aerial, terrestrial) for extracting

point clouds from images (Pierrot-Deseilligny and Clery, 2011). The pipeline of the software (Rupnik et al., 2017) is quite different comparing to the commercial one since all the commands in the employed version (5348 for Ubuntu) need to be inserted by the terminal. In the following points, a short list of the used simplified tools is reported :

- The first used tool was Tapioca, with this command MicMac computing the tie points on the images. The options that could be used in Tapioca are the strategy for extracting the information from the images (All, MulScale etc..) and the number of pixel that we need to use for extracting the tie points. In the present test all the possible pairs were analysed (options All) and in order to speed up the process the images were resampled at 1500 pixel (another option decided during the process).
- After Tapioca only the tie points are extracted, to align the images according to the extracted points another tool need to be launch: Tapas. This command allows to calibrate the images and to align it in a local reference system according to several parameters. A simple use of Tapas has been carried out using as calibration model the Fraser approach (Fraser, 1997). This is a radial model, with decentric and affine parameters the model has 12 degrees of freedom: 1 for focal length, 2 for principal point, 2 for distortion centre, 3 for coefficients of radial distortion (r3, r5, r7), 2 for decentric parameters, 2 for affine parameters, in this calibration model the PPA (Principal Point of Autocollimation) and PPS (Principal Point of Simmetry) are considered not equal. The next step was the image-point measurements. This part was performed in two steps using an approach similar to the one used in Context Capture: first of all, using three GCPs in three different images a rigid registration was performed (using SaisieAppuisInit for image measurements and GCPBascule for the rigid registration). Starting from this first results an accurate measurement of the other points has been achieved (SaisieAppuisPredict), the average number of measurements per marker was 18 with a minimum of 12 for CV10 and a maximum of 30 for CV17.
- Finally, for performing the BBA the weighting factor for the two components was fixed at 1 cm (is not possible in MicMac adopt different weight for the horizontal and vertical components). For image-coordinates of manually-measured markers the accuracy was set at $\frac{1}{2}$ of the pixel size. During the BBA in MicMac as interior

calibration parameters the ones derived from the first orientation process were used.

4 BUNDLE BLOCK ADJUSTMENT RESULTS

The quality of aerial triangulation was mainly evaluated by assessing the differences between the photogrammetrically-measured and the ground-surveyed object-coordinates of GCPs and CPs. Outlier rejection was preliminary performed, based on robust statistics, by means of an in-house Matlab

tool developed at the University of Pavia. For each component, X, Y and Z, the average value m of the residual was determined by means of the median operator. The standard deviation σ was also estimated, by multiplying the MAD (Mean Absolute Deviation) of the residuals by the factor 1.4826 (Hampel, 1974). The confidence interval was determined, having the form $[m - n \cdot \sigma, m + n \cdot \sigma]$, where the n coefficient was set at 2.5758, corresponding to the 99% probability under the normality condition. It must be said that all the measurements considered resulted to be inliers.

Table 2: Main statistical figures for GCP/CP residuals for Configuration 1.

Config 1: GCP 18		GCP			CP		
		X [m]	Y [m]	Z [m]	X [m]	Y [m]	Z [m]
Photoscan	mean	0.000	0.000	0.000	-	-	-
	std	0.003	0.003	0.009	-	-	-
	rmse	0.003	0.003	0.009	-	-	-
UAS Master	mean	0.000	0.000	0.000	-	-	-
	std	0.003	0.002	0.008	-	-	-
	rmse	0.003	0.002	0.008	-	-	-
Pix4D	mean	0.000	0.000	-0.001	-	-	-
	std	0.004	0.005	0.010	-	-	-
	rmse	0.004	0.005	0.010	-	-	-
Context Capture	mean	0.000	0.000	0.000	-	-	-
	std	0.004	0.004	0.009	-	-	-
	rmse	0.004	0.004	0.009	-	-	-
MicMac	mean	0.000	0.000	0.000	-	-	-
	std	0.002	0.002	0.002	-	-	-
	rmse	0.002	0.002	0.002	-	-	-

Table 3: Main statistical figures for GCP/CP residuals for Configuration 2.

Config 2: GCP 11/CP 7		GCP			CP		
		X [m]	Y [m]	Z [m]	X [m]	Y [m]	Z [m]
Photoscan	mean	0.000	0.000	0.000	-0.001	-0.001	-0.001
	std	0.003	0.003	0.009	0.004	0.005	0.013
	rmse	0.003	0.003	0.009	0.004	0.005	0.013
UAS Master	mean	0.000	0.000	0.000	0.002	-0.001	0.010
	std	0.003	0.003	0.008	0.007	0.004	0.017
	rmse	0.003	0.003	0.008	0.007	0.004	0.020
Pix4D	mean	0.000	0.000	-0.001	0.002	0.002	0.003
	std	0.004	0.005	0.008	0.005	0.007	0.015
	rmse	0.004	0.005	0.008	0.005	0.007	0.015
Context Capture	mean	0.001	-0.001	0.000	0.001	-0.002	-0.003
	std	0.005	0.004	0.009	0.009	0.007	0.012
	rmse	0.005	0.004	0.009	0.009	0.007	0.012
MicMac	mean	0.000	0.000	0.002	-0.004	0.005	0.047
	std	0.005	0.006	0.010	0.007	0.011	0.083
	rmse	0.005	0.006	0.011	0.008	0.012	0.096

Table 4: Main statistical figures for GCP/CP residuals for Configuration 3.

Config 3: GCP 6/CP 12		GCP			CP		
		X [m]	Y [m]	Z [m]	X [m]	Y [m]	Z [m]
Photoscan	mean	0.000	0.000	0.000	-0.001	-0.005	-0.007
	std	0.001	0.004	0.006	0.004	0.004	0.016
	rmse	0.001	0.004	0.006	0.004	0.006	0.017
UAS Master	mean	0.000	-0.001	0.002	0.001	0.00	0.007
	std	0.007	0.005	0.015	0.005	0.004	0.023
	rmse	0.007	0.005	0.015	0.005	0.004	0.024
Pix4D	mean	0.000	0.001	-0.001	-0.001	0.001	0.002
	std	0.004	0.008	0.008	0.005	0.005	0.014
	rmse	0.004	0.008	0.008	0.005	0.005	0.014
Context Capture	mean	-0.003	0.002	0.011	-0.007	0.000	0.020
	std	0.007	0.005	0.027	0.009	0.007	0.037
	rmse	0.008	0.005	0.029	0.011	0.007	0.042
MicMac	mean	0.000	-0.001	0.002	0.000	0.003	0.056
	std	0.003	0.005	0.012	0.015	0.017	0.090
	rmse	0.003	0.005	0.012	0.015	0.017	0.106

Table 5: Main statistical figures for GCP/CP residuals for Photoscan.

Photoscan		GCP			CP		
		X [m]	Y [m]	Z [m]	X [m]	Y [m]	Z [m]
Config 1 [GCP:18/18]	mean	0.000	0.000	0.000	-	-	-
	std	0.003	0.003	0.009	-	-	-
	rmse	0.003	0.003	0.009	-	-	-
Config 2 [GCP:11/11; CP:7/7]	mean	0.000	0.000	0.000	-0.001	-0.001	-0.001
	std	0.003	0.003	0.009	0.004	0.005	0.013
	rmse	0.003	0.003	0.009	0.004	0.005	0.013
Config 3 [GCP:6/6; CP:12/12]	mean	0.000	0.000	0.000	-0.001	-0.005	-0.007
	std	0.001	0.004	0.006	0.004	0.004	0.016
	rmse	0.001	0.004	0.006	0.004	0.006	0.017

Table 6: Main statistical figures for GCP/CP residuals for UAS Master.

UAS Master		GCP			CP		
		X [m]	Y [m]	Z [m]	X [m]	Y [m]	Z [m]
Config 1 [GCP:18/18]	mean	0.000	0.000	0.000	-	-	-
	std	0.003	0.002	0.008	-	-	-
	rmse	0.003	0.002	0.008	-	-	-
Config 2 [GCP:11/11; CP:7/7]	mean	0.000	0.000	0.000	0.002	-0.001	0.010
	std	0.003	0.003	0.008	0.007	0.004	0.017
	rmse	0.003	0.003	0.008	0.007	0.004	0.020
Config 3 [GCP:6/6; CP:12/12]	mean	0.000	-0.001	0.002	0.001	0.00	0.007
	std	0.007	0.005	0.015	0.005	0.004	0.023
	rmse	0.007	0.005	0.015	0.005	0.004	0.024

Table 7: Main statistical figures for GCP/CP residuals for Pix4D.

Pix4D		GCP			CP		
		X [m]	Y [m]	Z [m]	X [m]	Y [m]	Z [m]
Config 1 [GCP:18/18]	mean	0.000	0.000	-0.001	-	-	-
	std	0.004	0.005	0.010	-	-	-
	rmse	0.004	0.005	0.010	-	-	-
Config 2 [GCP:11/11; CP:7/7]	mean	0.000	0.000	-0.001	0.002	0.002	0.003
	std	0.004	0.005	0.008	0.005	0.007	0.015
	rmse	0.004	0.005	0.008	0.005	0.007	0.015
Config 3 [GCP:6/6; CP:12/12]	mean	0.000	0.001	-0.001	-0.001	0.001	0.002
	std	0.004	0.008	0.008	0.005	0.005	0.014
	rmse	0.004	0.008	0.008	0.005	0.005	0.014

Table 8: Main statistical figures for GCP/CP residuals for Context Capture.

zContext Capture		GCP			CP		
		X [m]	Y [m]	Z [m]	X [m]	Y [m]	Z [m]
Config 1 [GCP:18/18]	mean	0.000	0.000	0.000	-	-	-
	std	0.004	0.004	0.009	-	-	-
	rmse	0.004	0.004	0.009	-	-	-
Config 2 [GCP:11/11; CP:7/7]	mean	0.001	-0.001	0.000	0.001	-0.002	-0.003
	std	0.005	0.004	0.009	0.009	0.007	0.012
	rmse	0.005	0.004	0.009	0.009	0.007	0.012
Config 3 [GCP:6/6; CP:12/12]	mean	-0.003	0.002	0.011	-0.007	0.000	0.020
	std	0.007	0.005	0.027	0.009	0.007	0.037
	rmse	0.008	0.005	0.029	0.011	0.007	0.042

Table 9: Main statistical figures for GCP/CP residuals for MicMac.

MicMac		GCP			CP		
		X [m]	Y [m]	Z [m]	X [m]	Y [m]	Z [m]
Config 1 [GCP:18/18]	mean	0.000	0.000	0.000	-	-	-
	std	0.002	0.002	0.002	-	-	-
	rmse	0.002	0.002	0.002	-	-	-
Config 2 [GCP:11/11; CP:7/7]	mean	0.000	0.000	0.002	-0.004	0.005	0.047
	std	0.005	0.006	0.010	0.007	0.011	0.083
	rmse	0.005	0.006	0.011	0.008	0.012	0.096
Config 3 [GCP:6/6; CP:12/12]	mean	0.000	-0.001	0.002	0.000	0.003	0.056
	std	0.003	0.005	0.012	0.015	0.017	0.090
	rmse	0.003	0.005	0.012	0.015	0.017	0.106

Results are shown here, grouped in two different ways, to favourite analysis and comparisons. Tables 2-4 group results per configuration. Table 2 shows, for instance, results concerning GCPs and CPs for all the programs considered and only for Configuration 1. We show the name of the program used, the mean, standard deviation and RMSE of the difference between the photogrammetrically-obtained object-coordinates of markers and those determined by surveying; the analysis is performed for all the X, Y and Z components of GCPs and CPs, if any

Tables 5-9 illustrate the behaviour of the same program through the configurations depicted. Table 5 shows, for instance, results concerning Photoscan for all the three scenarios. We report the name of the configuration with the number of the GCPs and CPs used, the mean, standard deviation and RMSE values as explained above.

Figure 8 graphically summarizes results for the three configurations and five programs, in terms of RMSE. For readability reason, the axis of ordinates of the second and third graph is limited to 4.5 cm, while altimetric results for MicMac are larger, around 10 cm.

The figures shown suggest several remarks, some straightforward and others surprising.

- Horizontal components always perform better than Z. The only exception is constituted by MicMac in Configuration 1, where all coordinates show the same accuracy.
- It is well known that BBA estimates the orientation parameters in order to reach the best fitting between the photogrammetric and topographic coordinates of GCPs. A widely accepted rule states that accuracy figures for GCPs underestimate the actual ones. Therefore, it is useful and recommended to use independent check points in order to perform a reliable accuracy assessment. Our results confirm the mentioned general rule, but discrepancies between GCPs and CPs (for Configuration 2 and 3, only) are less evident than expected, especially for the planimetric components. This probably means that the statistics on GCPs can be considered a good quality estimator, at least for X and Y coordinates.
- The decreasing number of GCPs influences results, as expected. The different programs considered behave in a different way, according to this aspect. Photoscan, UAS Master and Pix4D always show good results while Context Capture has significant quality degradation in the altimetric component when passing from 11 to 6 GCPs (Table 8). Furthermore, the program shows anomalous values for Z in Configuration 3. Mic-

Mac presents good results for X and Y components but large residuals for Z, probably this aspect is connected to the calibration model used in MicMac. A strategy more similar to the one performed by the other used programs, like the FraserBasic model with PPA=PPS, should be reconsider as a best option where a little number of GCPs are used for the BBA.

- The GSD for the considered imagery is around 1.8 cm and is represented with a red dashed line in the figures. RMSE values are almost always

below the GSD value, thus highlighting that results are good in general. In Configuration 1, RMSE figures are all below the GSD threshold, for all the components and the programs adopted. Configuration 2 shows similar results also for altimetric component with an exception for MicMac software. In Configuration 3, all RMSE figures are within the GSD threshold apart from the Z component for ContextCapture (for both GCPs and CPs) and the Z of CPs for MicMac.

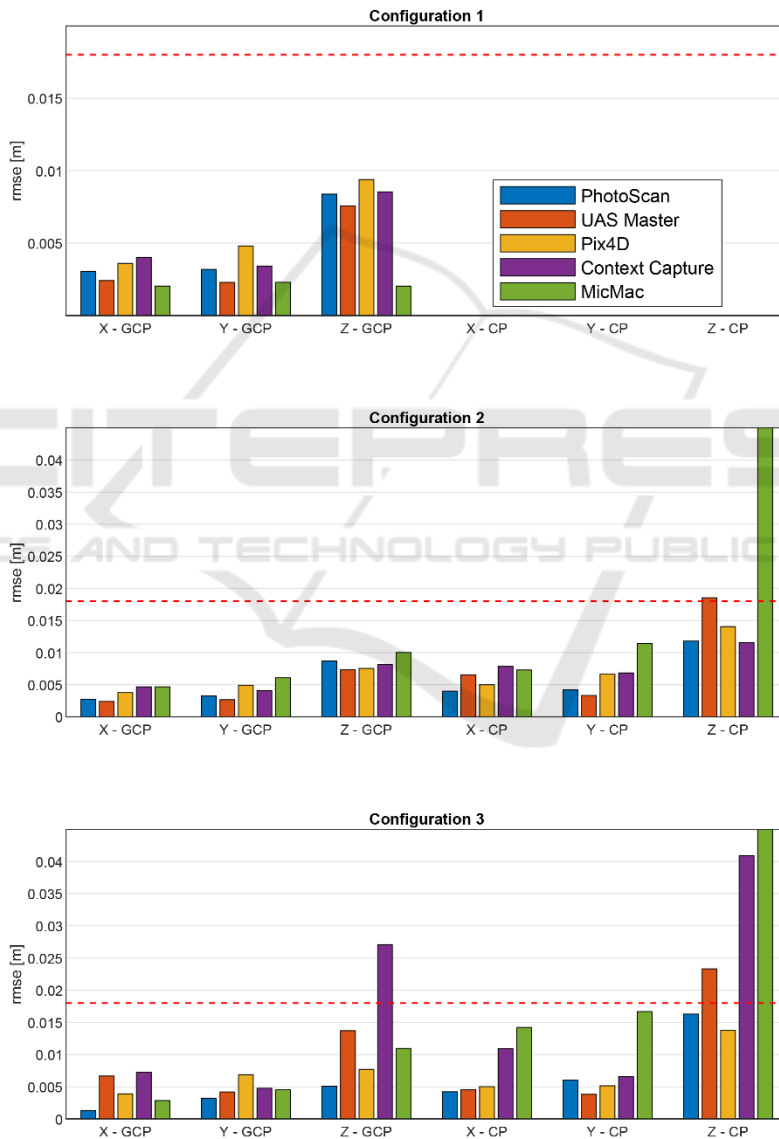


Figure 8: A summary of the obtained results. Histograms show the RMSE for the three-considered configurations; bars are coloured according to the software and the red dashed line represents the GSD value. The y-axis of Configuration 2 and 3 is limited to 4.5 cm for readability reason while the altimetric results on CPs for MicMac are larger.

5 CONCLUSIONS AND FURTHER ACTIVITIES

A significant part of a sandpit was surveyed by a UAV equipped with a Sony A6000 camera. A set of ground points were measured and used either for block orientation or quality assessment.

Five software were compared: Photoscan, UAS Master, Pix4D, Context Capture and MicMac. They were used to perform BBA in three configurations characterized by a different ratio between GCPs and CPs. In Configuration 1, markers were all used as GCPs to perform robust camera calibration; Configuration 2 deals with an intermediate setup with strong ground control and some check points; Configuration 3 is the more realistic one and simulates a routine surveying.

For each program, BBA strategy was carefully studied and final settings, described in Section 3, were tuned to optimize results. Residuals between the photogrammetrically-obtained object-coordinates of markers and those determined by surveying were formed and analysed.

Results for Photoscan, Pix4D and UAS Master are good, less than 1 GSD for the planimetric components and less than 1.5 GSD, at worst, for the altimetric one. Context Capture shows similar results for X and Y while the Z coordinate presents larger residuals especially for Configuration 3. Finally, MicMac shows anomalous residuals in the altimetric component for both Configuration 2 and 3; such values will be further investigated, using different calibration strategies to better evaluate the results in more similar conditions.

The decreasing number of GCPs influences results, as expected. Photoscan, UAS Master and Pix4D always show good results while Context Capture and MicMac present good results for X and Y components but large residuals for Z.

Further activities will follow two directions. On one hand, the other flights described in Table 1 will be processed with attention on oblique blocks to investigate their influence on final accuracy. On the other, final products, such as dense point clouds, will be assessed to explore the influence of BBA parameters in their generation. Several check points (more than 250) were already measured with a topographic total station on the upper flat area and on the scarp of the sandpit. An accurate comparison between the achieved point clouds and these points will be performed. Finally, an evaluation of point density will be realized comparing the clouds obtained in flat or scarp areas.

ACKNOWLEDGEMENT

The VAGA Srl company, being the owner of the surveyed sandpit, is here acknowledged for hosting the test. We are pleased to mention Eng. Emanuele Della Pasqua, Dr. Enrico Parmini, Dr. Maurizio Visconti, Surveyor Andrea Montemartini.

We are also pleased to thank two technicians of the Laboratory of Geomatics, Paolo Marchese and Giuseppe Girone for strongly supporting some phases of the described test: the manufacturing, placing and surveying of the markers, UAV management and data acquisition.

The authors' contribution was equal in the definition and drafting of the article. The processing was conducted in a coordinated but independent way by the two universities involved, as illustrated in Section 3.

REFERENCES

- Benassi, F., Dall'Asta, E., Diotri, F., Forlani, G., Morra di Cella, U., Roncella, R., Santise, M., 2017. Testing accuracy and repeatability of UAV blocks oriented with GNSS-supported aerial triangulation. In *Remote Sensing*, 9(2), 172.
- Casella, V., Franzini, M., 2016. Modelling steep surfaces by various configurations of nadir and oblique photogrammetry. In *ISPRS Annals of Photogrammetry, Remote Sensing and Spatial Information Sciences*, 3(1).
- Fraser, C., 1997. Digital camera self-calibration. In *ISPRS Journal of Photogrammetry and Remote Sensing*, vol. 52, issue 4, pp. 149-159
- Gini, R., Pagliari, D., Passoni, D., Pinto, L., Sona, G., Dosso, P., 2013. UAV photogrammetry: Block triangulation comparisons. In *Int. Arch. Photogram. Remote Sens. Spat. Inf. Sci.*, 1, W2.
- Hampel, F.R., 1974. The influence curve and its role in robust estimation. In *Journal of the American statistical association*, 69(346), 383-393.
- James, M. R., Robson, S., d'Oleire-Oltmanns, S., Niethammer, U., 2017. Optimising UAV topographic surveys processed with structure-from-motion: Ground control quality, quantity and bundle adjustment. In *Geomorphology*, 280, 51-66.
- Lucieer, A., Jong, S.M.D., Turner, D., 2014. Mapping landslide displacements using Structure from Motion (SfM) and image correlation of multi-temporal UAV photography. In *Progress in Physical Geography*, 38(1), 97-116.
- Nex, F., Remondino, F., 2014. UAV for 3D mapping applications: a review. In *Applied geomatics*, 6(1), 1-15.
- Nocerino, E., Menna, F., Remondino, F., Saleri, R., 2013. Accuracy and block deformation analysis in automatic UAV and terrestrial photogrammetry-Lesson learnt. In

- ISPRS Annals of the Photogrammetry, Remote Sensing and Spatial Information Sciences*, 2(5/W1), 203-208.
- Pierrot-Deseilligny, M., Clery, I., 2011. APERO, an Open Source Bundle Adjustment Software for Automatic Calibration and Orientation of a Set of Images. In *ISPRS Archives*, International Workshop 3D-ARCH, on CD-ROM, Trento, Italy
- Rangel, J. M. G., Gonçalves, G. R., Pérez, J. A., 2018. The impact of number and spatial distribution of GCPs on the positional accuracy of geospatial products derived from low-cost UASs. In *International journal of remote sensing*, 39(21), 7154-7171.
- Remondino, F., Barazzetti, L., Nex, F., Scaioni, M., Sarazzi, D., 2011. UAV photogrammetry for mapping and 3d modeling—current status and future perspectives. In *International Archives of the Photogrammetry, Remote Sensing and Spatial Information Sciences*, 38(1), C22.
- Rupnik, E., Daakir, M., Deseilligny, M. P., 2017. MicMac—a free, open-source solution for photogrammetry. In *Open Geospatial Data, Software and Standards*, 2(1), 14.
- Samad, A.M., Kamarulzaman, N., Hamdani, M.A., Mastor, T. A., Hashim, K.A., 2013. The potential of Unmanned Aerial Vehicle (UAV) for civilian and mapping application. In *System Engineering and Technology (ICSET)*, 2013 IEEE 3rd International Conference on, 313-318.
- Tahar, K. N., 2013. An evaluation on different number of ground control points in unmanned aerial vehicle photogrammetric block. In *Int. Arch. Photogramm. Remote Sens. Spat. Inf. Sci.*, 40, 93-98.
- Verykokou, S., Ioannidis, C., Athanasiou, G., Doulamis, N., Amditis, A., 2018. 3D reconstruction of disaster scenes for urban search and rescue. *Multimedia Tools and Applications*, 77(8), 9691-9717.
- Zongjian, L.I.N., 2008. UAV for mapping-low altitude photogrammetric survey. In *International Archives of Photogrammetry and Remote Sensing*, Beijing, China, 37, 1183-1186.